Sensors and Actuators B 188 (2013) 1319–1327

Contents lists available at ScienceDirect

Sensors and Actuators B: Chemical

journal homepage: www.elsevier.com/locate/snb

Nonlocal mass nanosensors based on vibrating monolayer graphene sheets

T. Murmu [a,*], S. Adhikari [b,1]

[a] Department of Mechanical, Aeronautical and Biomedical Engineering, Irish Centre for Composites Research, Materials and Surface Science Institute, University of Limerick, Ireland
[b] Multidisciplinary Nanotechnology Centre, Swansea University, Singleton Park, Swansea SA2 8PP, UK

ARTICLE INFO

Article history:
Received 22 March 2013
Received in revised form 13 July 2013
Accepted 15 July 2013
Available online xxx

Keywords:
Nanosensors
Nonlocal elasticity
Sensor relations
Molecular mechanics

ABSTRACT

Single layer graphene sheets (SLGS) as a nanoscale label-free mass sensor are proposed. A mathematical framework according to nonlocal elasticity is considered. The nonlocal elasticity incorporates the small-scale effects or nonlocality in the analysis. Rectangular graphene resonators are assumed to be in cantilevered configuration. Closed-form nonlocal equations are derived for the frequency shift due to the added mass based on four types of different mass loadings. From the potential and kinetic energy of the mass loaded graphene sheets, generalised nondimensional calibration constants are proposed for an explicit relationship among the added mass, nonlocal parameter and the frequency shift. These equations based on nonlocal elasticity in turn are used for sensing the added mass (e.g. adenosine bio-fragment). Molecular mechanics simulation is used to validate the new nonlocal sensor equations. The optimal values of span of nonlocal parameter are used and compared with the molecular mechanics simulation results. The nonlocal approach generally predicts the frequency shift accurately compared to the local approach in most cases. Numerical results show the importance of considering the distributed nature of the added mass while using the nonlocal theory. The performance of the sensor is governed on the spatial distribution of the attached mass on the graphene sheet. Discussion on the numerical results illustrate that the sensitivity of graphene sensors is in the order of Gigahertz/zeptogram.

1. Introduction

Recently graphene [1,2] has attracted huge attention among the scientific and nanotechnological communities. The graphene, a basic structure for graphitic materials of all dimensionalities, is a single layer of carbon atoms packed into a two-dimensional honeycomb lattice [3]. Graphene sheets may be single-layer (SL) [4] atomic thick or multilayer [5] consisting of several SL graphene sheets.

The electronic properties of graphene nanoribbons defined by their quasi-one-dimensional electronic confinement [6] indicate remarkable applications in graphene-based devices. Graphene has parallels with many properties of carbon nanotubes (CNTs) [7]. However, due to their planner structure, some of the properties seem to be easier to handle than CNTs. Graphene has many potential area of applications [8]. Applications of graphene include composites for windmill blades and aircraft components, low cost efficient solar cells [9], high frequency transistors, hydrogen storage [10], ultracapacitors, faster recharging batteries, display in mobile devices, energy harvesting [11].

Detection systems or sensors are important instruments. Sensors at nanoscale are devices that detect small number of molecules/atoms of gas, biological and chemicals objects needed to be detected. This is upon consideration with least amount of change in some measured quantity. It measures the desired physical quantity and converts it into required parameter. The detection of presence of chemical and biological molecules with high sensitivity and selectivity is crucial in various fields. Some practical area of sensing and detection comprises detection of gas leakage, diagnosis of diseases and health care.

Sensors are of different types, and among the various types of sensors; solid state sensors have received significant attention. These sensors include solid electrolyte sensors [12], catalytic sensors [13], bio sensor [14] and semiconducting oxide gas sensors. With the advent of nanotechnology, a new class of sensors were developed based on the utilisation of fullerene, graphene and carbon nanotubes (CNT). Electronic sensors fabricated of fullerene are very sensitive to any adsorbed molecule. The sensitivity of CNT based sensors can be enhanced by controlling the defect sites as electron transport through CNT is influenced by the functionalisation of side walls of CNT. After the recent discovery of graphene [1], a completely new area has opened that

* Corresponding author.
E-mail addresses: murmutony@gmail.com (T. Murmu), s.adhikari@swansea.ac.uk (S. Adhikari).
[1] Tel.: +44 01792 602969; fax: +44 01792 295676.

0925-4005/$ – see front matter © 2013 Elsevier B.V. All rights reserved.
http://dx.doi.org/10.1016/j.snb.2013.07.051

promises ultra-sensitive and ultra-fast electronic sensor devices due to being low electrical noise material [15]. Further having superior electronic properties, graphene offers large surface area, high flexibility and biocompatibility and good facile chemical functionalisation which brands it as efficient sensing element. Graphenes are also important for sensor applications such as for diagnosis of diseases [16]. In graphene sensors, the molecules that are sensitive to particular diseases can attach to the carbon atoms in graphene. The graphene sheets can also be employed as chemical sensors effective at detecting explosives [17]. These sensors enclose sheets of graphene in the form of foam which affects the resistance when low levels of vapours from chemicals are present. Graphene is also used as potential mass sensors and dust detectors [18], gas sensors [19,20], electrochemical sensors [21], pressure nanosensors [22], magnetic field sensor [23].

The mechanical behaviour of graphene sheets are analysed and understood by experimental methods, molecular dynamics simulations [24,25] and continuum mechanics. Within continuum mechanics, size-dependant theories [26] are quite popular as it yields faster and reasonable predictions with less resource. One widely used size-dependant continuum theory for the mechanical analysis of graphene sheets is the nonlocal elasticity theory pioneered by Eringen [27].

At nanometre scales, surface and size effects often become prominent and cannot be ignored. Both experimental and atomistic simulation results have shown a significant size-effect [24,28–30] in the mechanical properties when the dimensions of these structures become small. The theory of nonlocal elasticity accounts for the small-scale (size) effects at the atomistic level; and can also account for macro structures. Size-effects are associated to atoms and molecules that constitute the materials. Computational methods such as molecular dynamic (MD) simulation are reasonable in the analysis of nanostructures [4], however the approach is computationally exorbitant for nanostructures with large numbers of atoms. This asks for the usage of conventional continuum mechanics [5] applied in analysis of macro structures. Classical continuum models are considered scale-free and it lacks the accountability of the effects arising from the small-scale where 'size-effects' are prominent. The application of classical continuum models may be questionable in the analysis of nanostructures such as carbon nanotubes and graphene sheets. One popular size-dependant continuum theory is the nonlocal elasticity theory pioneered by Eringen [27] which bring in the scale-effects and physics within the formulation. The theory of nonlocal elasticity finds general application in the area of nanostructural study such as in nanorods [31], nanobeams [32], nanoplates [33], nanorings [34], carbon nanotubes [35], graphenes [36], nanoswitches [37] and protein microtubules [38]. Via nonlocal elasticity theory the small-scale effects are incorporated by assuming that the stress at a point as a function of the strains at all points in the domain. Nonlocal theory considers long-range inter-atomic interaction and yields results dependent on the size of a body. Some of the drawbacks of the classical continuum theory (such as beam and plate theories) could be efficiently avoided and size-dependent phenomena can be clarified by the nonlocal elasticity theory. A good review on nonlocal elasticity and application to nanostructures (CNTs and graphene) is reported in Ref. [39].

Though nonlocal elasticity theory is an important analytical theory for nanoscale structures, it has been scarcely used for sensor analysis. Lee et al. [40] has proposed carbon-nanotube-based cantilever sensor with an attached mass using frequency analysis and nonlocal elasticity theory. Analytical sensor equations were provided. Mathematical relationship between the frequency shift of the sensor and the attached mass were obtained. The double-walled carbon nanotube (DWCNT) as micromass sensor using nonlocal Timoshenko beam vibration theory was explored by Shen et al. [41]. The results were also compared with finite element method considering no nonlocal effects. It was also reported that the nonlocal Timoshenko beam model is more accurate than the nonlocal Euler–Bernoulli beam model for short DWCNT sensors. Considering flexural vibration of nanotubes, sensor theories were developed [40,41]. Sensors based on nonlocal axial vibration are recently addressed. Aydogdu and Filiz [42] proposed carbon nanotube-based mass sensors based on axial vibration and nonlocal elasticity theory. The works above however have not been compared with molecular dynamics simulations. Murmu and Adhikari [14] have studied the carbon nanotube based cantilever bio sensor using nonlocal elasticity theory and vibration analysis. The nonlocal elastic formulations were compared with molecular mechanics simulations and optimal value of nonlocal parameter was proposed. According to their study the nonlocal approach generally predicts the frequency shift accurately compared to the local approach in most cases. Numerical results show the importance of considering the distributed nature of the added mass while using the nonlocal theory.

Based on nonlocal elasticity theory and vibration analysis, carbon nanotube based sensors are proposed. Very limited work on nonlocal graphene sensors are carried out. Shen et al. [43] illustrated the potential of resonating single-layered graphene sheet (SLGS) as a nanomechanical sensor using nonlocal Kirchhoff's plate theory. The effects of the mass and position of the nanoparticle on the frequency shift of the graphene sheet are discussed. The mathematical development of CNT and graphene based sensors via nonlocal elasticity is in its nascent stage, and further study is required for its realistic applications.

Resonance based sensors [44–46] offer significant potential of achieving the high-fidelity requirement of many sensing applications, and reaches very high resolutions. According to their Aydogdu and Filiz [42], theoretically the mass sensitivity of nanotube-based mass sensors can reach zeptograms. According to Ekinci et al. [47], theoretically, nanosensors can achieve ultimate mass sensitivity limits of 1 yg (1 yg = 10^{-24} g). Recently Chaste et al. [48] established the extreme sensitivity of mass sensing carbon nanotube sensor via experiments. Their experimental work showed that a resolution of 1.7 yg which corresponds to the mass of one proton, or one hydrogen atom can be achieved. Using the high resolution nanosensor of this type, different chemical elements in future inertial mass spectrometry measurements can be distinguished.

In resonance based sensors, the principle of mass detection employing resonators is based on the fact that the resonant frequency is sensitive to the resonator mass [45]. The resonator mass comprises the self-mass of the resonator and the attached mass. The variation of the attached (adsorbed) mass on the resonator causes a shift to the resonant frequency. The key issue of mass detection is in monitoring (quantifying) the change in the resonant frequency due to the added mass.

Nano-scale sensors and the nonlocal theory is a valid efficient theory for a wide range of nano-scale objects, in this paper we aim to put these together for SLGS sensor. Being one atom thick, graphene may either be in direct contact with substrate or would be suspended. Therefore interface state should play important role in sensing. Building and designing such nanosensors that is able to make measurements of external deposited agents with ultrahigh resolution is one of the main goals in the field of nanomechanics. In particular, we develop a new analytical approach for graphene sensor using nonlocal elasticity theory (Fig. 1). Graphene is modelled as nonlocal thin plate. We derive the updated calibration constants necessary for using single layer graphene sheet (SLGS) as nanomechanical resonators in nano sized mass sensors. Via nonlocal theory, natural vibration of SLGS with bio-fragment (e.g. adenosine) is discussed in Section 2. Four types of mass loadings are considered and

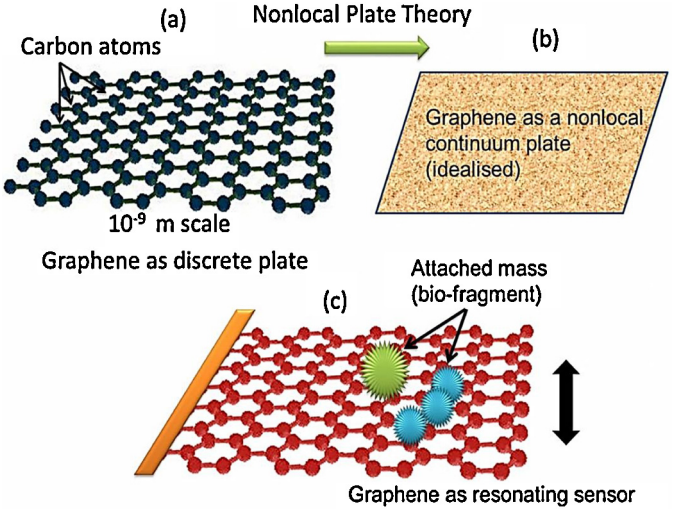

Fig. 1. (a) Schematic diagram of single-layer graphene sheets, (b) nonlocal continuum plate as a model for graphene sheets, (c) resonating graphene sheets sensors with attached bio fragment molecules such as adenosine.

closed-form equations have been derived for the frequency shift due to the added mass. Nonlocal sensor equations and sensitivity calculations are discussed in Section 3. A molecular mechanics approach based on the universal force field (UFF) model is used in Section 4 to validate the new results derived in the paper. The results obtained using the analytical approach is discussed for three cases of mass distributions. It is illustrated that the new sensor equations obtained using the proposed nonlocal theory can provide more accurate prediction of the attached mass compared to the same using the classical theory.

2. Natural vibration of SLGS with bio-fragment and small-scale effects

Various methods are used to investigate the vibration phenomenon of single and multiple layer graphene sheets. They include molecular mechanics method [49], equivalent lattice structures made by atomistic-continuum models representing the C—C bonds, classical continuum mechanics, modified couple stress theory [26]. Further the out-of-plane deformation of SLGS has been considered using the continuum mechanics models, together with continuum and truss-like structural assemblies.

In the present work, we consider thin nonlocal elastic plate model [43,50–54] for vibration analysis of single layer graphene sheets due to its simplicity. Conditions based on Kirchhoff's plate theories are assumed. Small-scale or nonlocal effects arising at atomic level are included in the formulation. According to nonlocal elasticity, the stress at a point is a function of the strains at all points in the domain. The stress at a point is defined as

$$\sigma_{ij}(x) = \int_V \phi(|x - x'|, \alpha) H_{ijkl} \varepsilon_{kl} dV(x'), \forall x \in V.$$

The terms σ_{ij}, ε_{kl}, H_{ijkl}, are the stress, strain and fourth-order elasticity tensors respectively. The integral equation couples the stress due to nonlocal elasticity and the stress due to classical elasticity. The kernel function $\phi(|x - x'|, \alpha)$ denotes the nonlocal modulus. The nonlocal modulus acts as an attenuation function incorporating into constitutive equations the nonlocal effects at the reference point x produced by local strain at the source x'. The nonlocal integral equation is difficult to solve, thus a differential equation is used [27].

Assuming the nonlocal thin plate (Fig. 1b) has dimension $c \times b$, the vibration equation can be expressed as [50]

$$D\nabla^4 u + m(1 - (e_0 a)^2 \nabla^2) \left\{ \frac{\partial^2 u}{\partial t^2} \right\} = 0, \qquad 0 \le x \le c; \quad 0 \le y \le b \tag{1}$$

Here $u = u(x, y, t)$ is the transverse deflection, $\nabla^2 = ((\partial/\partial x^2) + (\partial/\partial y^2))$ is the differential operator, x, y are coordinates, t is the time, m is the mass per unit area and the bending rigidity is defined by

$$D = \frac{Eh^3}{12(1 - \nu^2)} \tag{2}$$

E is the Young's modulus, h is the thickness and ν is the Poisson's ratio. For some practical device, a graphene layer would be supported on some kind of substrate. This would alter the bending rigidity in Eq. (2), if the proposed theory to be used. We consider rectangular graphene sheets with cantilevered (clamped at one edge) boundary condition (Fig. 1c). For single layer graphene sheets, the thickness is generally assumed as one atomic thick (though it can be scattered). It can be assumed as 0.34 nm. The term $e_0 a$ is the dimensional nonlocal parameter or scale coefficient. Term $e_0 a$ is a parameter associated with the material, where 'a' is the intrinsic characteristic length such as lattice parameter, distance between C—C atoms, granular length. Here e_0 is a constant for calibrating the model with experimental results and other validated models [27]. The parameter e_0 is estimated such that the relations of the nonlocal elasticity model could deliver satisfactory approximation to the atomic dispersion curves of the plane waves with those obtained from the atomistic lattice dynamics. According to Duan et al. [55] nonlocal parameter is not unique and depends on various parameter. Researchers are working to find an optimum value of nonlocal parameter for nanotubes and graphene sheets. For carbon nanotubes and graphene sheets, the $e_0 a$ is assumed in the range of 0–2.0 nm. One important way of obtaining the values of nonlocal parameter is by evaluating from the molecular dynamics simulation. Various values of nonlocal parameters as suggested by researchers are discussed in Ref. [56].

2.1. Vibration of SLGS without attached mass

In this section, we formulate the natural frequencies of vibration of SLGS without any attached masses. We consider cantilever boundary condition in our study. The study is primarily interested on the first vibration mode of the system.

The first natural frequency (in rad/s) of a rectangular plate of dimension $c \times b$ can be expressed as [57]

$$\omega_0^2 = \left(\frac{\pi^4 D}{c^4 \rho} \right) \frac{0.0313}{0.2268} \tag{3}$$

Here the graphene sheets are assumed to be in perfect planar configuration. According to Meyer et al. [58] spontaneous ripples and wrinkling are found on free-standing graphene sheets through vacuum between metal struts. Edge stress induced warping and instability are noticed using analytical [59], first principles study [60] and numerical methods [61]. Since the SLGS considered here is clamped at one edge, the substrate at the clamping edge may contain atomistic-scale defects resulting wrinkles along that edge. In this paper we have neglected the inaccuracies arising due to the wrinkling of SLGS.

The vibration mode-shape for the first mode of vibration of the planar SLGS is given by

$$w(x, y) = 1 - \cos\left(\frac{\pi x}{2c} \right) \tag{4}$$

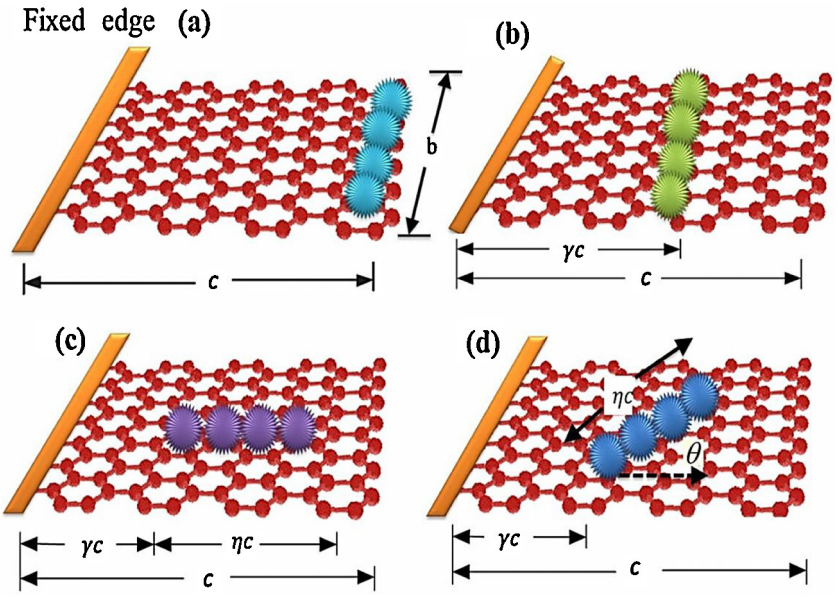

Fig. 2. (a) Masses at the cantilever tip in a line (b) masses in a line along the width, (c) masses in a line along the length, and (d) masses in a line with an arbitrary angle.

The natural frequency of the system can be alternatively obtained using the energy principle. Using variational and energy principles, Adali [62] has carried out analysis orthotropic graphene sheets embedded in an elastic medium. Assuming the harmonic motion, the kinetic energy of the nonlocal vibrating plate can be expressed by

$$T = \omega^2 \int_A w^2(x,y)\rho \mathrm{d}A + \omega^2 \int_A (e_0 a)^2 \{\nabla w(x,y)\}^2 \rho \mathrm{d}A \tag{5}$$

Here ω denotes the frequency of oscillation and A denotes the area of the graphene plate. Here $e_0 a$ is the nonlocal parameter as discussed above. We have neglected the nonlocality arising from the added mass. Using the expression of $w(x, y)$ in Eq. (4) we get

$$T = \frac{1}{2}\omega^2 (cb\rho)\left(\frac{3\pi - 8}{2\pi} + \frac{\mu^2\pi^2}{8}\right) \tag{6}$$

where the nondimensional length scale parameter (dimensionless nonlocal parameter)

$$\mu = \frac{e_0 a}{c} \tag{7}$$

The potential energy can be obtained as

$$U = \frac{D}{2}\int_A \left\{ \left(\frac{\partial^2 w}{\partial x^2} + \frac{\partial^2 w}{\partial y^2}\right) - 2(1-\nu) \left[\frac{\partial^2 w}{\partial x^2}\frac{\partial^2 w}{\partial y^2} - \left(\frac{\partial^2 w}{\partial x \partial y}\right)^2\right]\right\} \mathrm{d}A \tag{8}$$

Using the expression of $w(x, y)$ in (4) we have

$$U = \frac{D}{2}\rho \int_0^c \int_0^b \left(\frac{\partial^2 w}{\partial x^2}\right)^2 \mathrm{d}x\,\mathrm{d}y = \frac{1}{2}\frac{\pi^4 D}{c^3} b \left(\frac{1}{32}\right) \tag{9}$$

Considering the energy balance, that is $T_{\max} = U_{\max}$, from Eqs. (7) and (9) the resonance frequency can be obtained as

$$\omega_0^2 = \left(\frac{\pi^4 D}{c^4 \rho}\frac{1/32}{(3\pi - 8)/2\pi + \mu^2\pi^2/8}\right) \tag{10}$$

This matches reasonably well with the numerical value reported in Eq. (3) with consideration of small scale effects. Next, we calculate the kinetic energy due to additional attached mass and use the energy principle to obtain the modified resonance frequency.

2.2. Vibration of SLGS with attached mass

Because of the two dimensional nature of the graphene sheet, the SLGS resonator offers more flexibility in terms of attaching different types of molecules at different spatial locations. By exploiting the spatial spread of a two-dimensional graphene sheet, SLGS sensors can be designed such that it can effectively substitute an array of cantilever nanotube sensors. A two dimensional surface offers vast opportunities for attaching (adsorbing) molecules to the graphene sheet. Compared to carbon nanotubes, monolayer graphene resonators have the benefit of more larger surface area for the arrest of the additional mass [63]. As in Adhikari and Chowdhury [45], we have considered four possible arrangements by which bio-molecules can be attached with the graphene sheet. The four cases are: case (a): masses at the cantilever tip in a line; case (b): masses in a line along the width; case (c): masses in a line along the length; case (d): masses in a line with an arbitrary angle. Fig. 2 shows the schematic diagram of the four cases.

Apart from the four cases considered here, it is certainly possible to have different mass distributions. The method developed here is general and can be applied to more general cases if the geometry is known. The considered four cases in Fig. 2 are for development of the understanding on the behaviour of the proposed sensor for typical mass distributions and nonlocal effects.

From the practical standpoint, for label-free sensors it is generally not possible to a priori identify exactly the spatial location of the attached molecules. Techniques such as high resolution imaging can be employed to capture the spatial location of the attached molecules. Further, many nanomechanical biosensors practise specific coatings on the resonators to make them sensitive to particular biomolecules. Here, the sensor will not be label-free but the spatial location of the attachment region will be a priori known. The attachment region can even be optimally designed taking the shape and size of the molecules to be detected in to account. The analysis presented below is valid for both of these approaches as in Adhikari and Chowdhury [45]. The analytical results to be derived precisely quantify the effect of spatial location of the attached molecules (not just their mass) on the performance of the sensor.

2.2.1. Attached masses are at the cantilever tip

Let us consider the case when the attached masses are at the cantilever tip in a line as shown in Fig. 2(a). Assuming the total attached mass is M, the combined kinetic energy of the SLGS and the attached mass can be obtained as

$$T_a = \frac{1}{2}\omega^2 \left\{ \int_A [w^2(x,y)+(e_0a)^2\{\nabla w(x,y)\}^2]\rho\, dA + Mw^2(x,y)|_{x=a} \right\}$$
$$= \frac{1}{2}\omega^2 \left\{ M_g \left(\frac{3\pi-8}{2\pi} + \frac{\mu^2\pi^2}{8} \right) + M \right\} \quad (11)$$

where

$$M_g = \rho cb \quad (12)$$

is the mass of the graphene sheet. Considering the energy balance, that is $T_{max} = U_{max}$, from Eqs. (11) and (9) the resonance frequency can be obtained as

$$\omega_a^2 = \frac{(1/2)(\pi^4 D/c^3)b(1/32)}{1/2\{M_g(((3\pi-8)/2\pi)+(\mu^2\pi^2/8)+M)\}}$$
$$= \left(\frac{\pi^4 D}{c^4\rho} \right) \frac{1/32}{(3\pi-8)/2\pi + \mu^2\pi^2/8 + M/M_g} \quad (13)$$

From this equation we can see how the added mass M reduces the resonance frequency.

2.2.2. Attached masses arranged in a line along the width

Here we consider the case when the attached masses are arranged in a line along the width as shown in Fig. 2(b). It is assumed that the masses are at a distance of γc, $\gamma \le 1$, from the fixed edge of the graphene sheet. The kinetic energy of the system can be obtained as

$$T_b = \frac{1}{2}\omega^2 \left\{ \int_A [w^2(x,y)+(e_0a)^2\{\nabla w(x,y)\}^2]\rho\, dA + Mw^2(x,y)|_{x=\gamma c} \right\}$$
$$= \frac{1}{2}\omega^2 \left\{ M_g \left(\frac{3\pi-8}{2\pi} + \frac{\mu^2\pi^2}{8} \right) + M\alpha_b \right\} \quad (14)$$

where the factor

$$\alpha_b = \left(1 - \cos\left(\frac{\pi\gamma}{2} \right) \right)^2 \quad (15)$$

2.2.3. Attached masses arranged in a line along the length

For the case shown in Fig. 1(c), we consider that the length of the attached mass is ηc and its density along the length is uniform. We also consider that the mass is placed at a distance of γc from the fixed edge. Since the mass always rests within the graphene sheet, both $\gamma \le 1$, $\eta \le 1$ and additionally $\gamma + \eta \le 1$. The kinetic energy of the system with nonlocal effects can be obtained as

$$T_c = \frac{1}{2}\omega^2 \left\{ \int_A [w^2(x,y) + (e_0a)^2\{\nabla w(x,y)\}^2]\rho\, dA + \int_{\gamma a}^{(\gamma+\eta)c} \frac{M}{\eta a} w^2(x,y)dx \right\}$$
$$= \frac{1}{2}\omega^2 \left\{ M_g \left(\frac{3\pi-8}{2\pi} + \frac{\mu^2\pi^2}{8} \right) + M\alpha_c \right\} \quad (16)$$

where by calculating the above integral one has

$$\alpha_c = \frac{3\pi\eta + [\sin((\gamma+\eta)\pi) - \sin(\gamma\pi)] - 8[\sin((\gamma+\eta)\pi/2) - \sin(\gamma\pi/2)]}{2\pi\eta} \quad (17)$$

In the above expression use M as the mass per unit length of the attached object.

2.2.4. Attached masses arranged with arbitrary angle

The most general case of the attached object is that arranged in an arbitrary angle and is shown in Fig. 2(d). Depending on the value of θ, it reduces to the earlier two previous cases. The values of γ and η should be such that the mass remains within the graphene sheet. This implies that $\gamma + \eta\cos(\theta) \le 1$ and $\eta c \le b\cos(\theta)$. Considering the mass per unit length along the x-axis as M, kinetic energy with nonlocal effects of the system can be obtained as

$$T_d = \frac{1}{2}\omega^2 \left\{ \int_A [w^2(x,y) + (e_0a)^2\{\nabla w(x,y)\}^2]\rho\, dA + \int_{\gamma a}^{(\gamma+\eta\cos(\theta))c} \frac{M}{\eta a\cos(\theta)} w^2(x,y)dx \right\}$$
$$= \frac{1}{2}\omega^2 \left\{ M_g \left(\frac{3\pi-8}{2\pi} + \frac{\mu^2\pi^2}{8} \right) + M\alpha_c \right\} \quad (18)$$

where

$$\alpha_d = \frac{3\pi\eta\cos(\theta) + [\sin((\gamma+\eta\cos(\theta))\pi) - \sin(\gamma\pi)] - 8[\sin((\gamma+\eta\cos(\theta))\pi/2) - \sin(\gamma\pi/2)}{2\pi\eta\cos(\theta)} \quad (19)$$

Taking the limit $\theta \to \pi/2$ and $\theta \to 0$, Eq. (18) reduces to Eqs. (14) and (16) respectively. The resonance frequency corresponding to cases (b)–(d) can be obtained using the energy principle used for case (a). Considering the energy balance, the resonance frequency can be expressed in a general form as

$$\omega_{b,c,d}^2 = \frac{(1/2)(\pi^4 D/c^3)b(1/32)}{1/2\{cb\rho((3\pi-8)/(2\pi)+(\mu^2\pi^2/8))+\alpha_{b,c,d}M\}}$$
$$= \left(\frac{\pi^4 D}{c^4\rho} \right) \frac{1/32}{(3\pi-8)/2\pi + \mu^2\pi^2/8 + \beta\alpha_{b,c,d}} \quad (20)$$

Here the ratio of the added mass

$$\beta = \frac{M}{M_g} \quad (21)$$

and $\alpha_{b,c,d}$ are factors which depend on the mass distribution as defined before.

3. Sensor equations and sensitivity analysis

For notational convenience, we express the natural frequency of the mass loaded graphene sheet as

$$\omega_\eta^2 = \left(\frac{\pi^4 D}{c^4\rho} \right) \frac{1/32}{(3\pi-8)/2\pi + \mu^2\pi^2/8 + \beta\alpha_n} \quad (22)$$

where α_n stands for different values of α, which in turn depend on the distribution of the attached mass. Taking the ratio with the resonance frequency of the graphene sheet without any mass in (10), we have

$$\frac{\omega_n}{\omega_0} = \frac{1}{\sqrt{1+c_n\beta}} \quad (23)$$

Here the calibration constant c_n is given by

$$c_n = \frac{8\pi\alpha_n}{4(3\pi-8)+\mu^2\pi^3} \quad (24)$$

Considering $\omega = 2\pi f$, the frequency shift in Hz due to the added mass can be obtained as

$$\Delta f = f_0 - f_n = 2\pi(\omega_0 - \omega_n) \quad (25)$$

The relative frequency shift can be obtained from (25) as

$$\frac{\Delta f}{f_0} = 1 - \frac{1}{\sqrt{1+c_n\beta}} \quad (26)$$

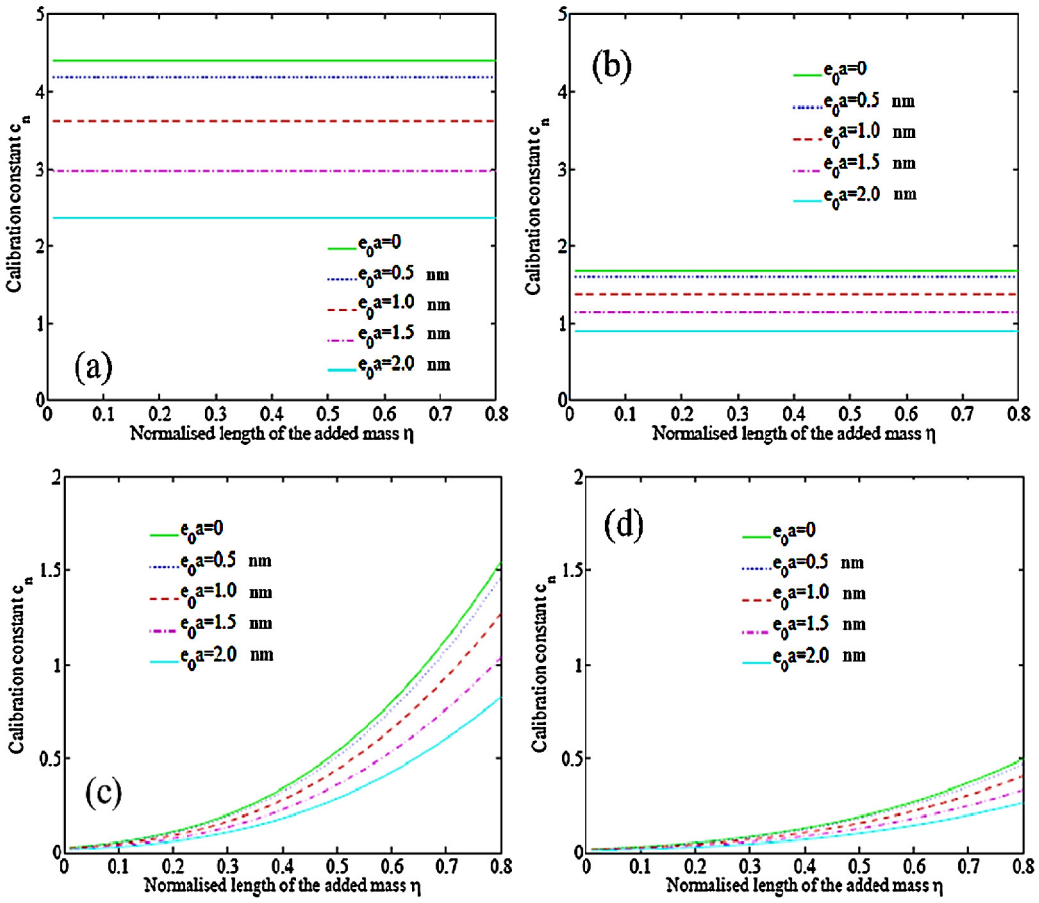

Fig. 3. Calibration constants corresponding to four cases. (a) Case (a): Masses at the cantilever tip in a line and is independent of γ and η; (b) case (b): masses in a line along the width and the value of $\gamma = 0.75$ is considered; (c) case (c): masses in a line along the length and the value of $\gamma = 0.25$ and the normalised length η is varied between 0 and 0.75; (d) case (d): masses in a line with an arbitrary angle. The value of angle $\theta = \pi/4$ and rest of the values are kept same as case (c). The length of the SLGS is assumed to be 5 nm for the purpose of calculating $\mu = e_0a/L$.

Using this expression, the relative added mass of the bio-fragment can be found from the frequency shift as

$$\beta = \frac{1}{c_n(1-(\Delta f/f_0))^2} - \frac{1}{c_n} \tag{27}$$

The normalised sensitivity of the graphene based sensor can be obtained by the differentiation of Eq. (26) as

$$\frac{\partial(\Delta f/f_0)}{\partial\beta} = \frac{c_n}{2(1+c_n\beta)^{3/2}} \tag{28}$$

The dimensional sensitivity (in Hz/g) can be obtained from Eq. (28) as

$$\frac{\partial(\Delta f)}{\partial M} = \frac{f_0}{M_g}\frac{c_n}{2}(1+c_n\beta)^{-3/2} \tag{29}$$

The absolute maximum sensitivity of a grapheme based sensor therefore given by

$$\frac{\partial(\Delta f)}{\partial M}|_{\max} = \frac{f_0}{M_g}\frac{c_n}{2} \tag{30}$$

This implies that for a given graphene sheet, the higher value of c_n will result in a sensor with higher sensitivity. The four calibration constants presented are plotted for different values of the normalised length η in Fig. 3 and nonlocal parameter e_0a.

The nonlocal parameter is taken in the range 0–2 nm. Among the four cases considered here, case (a), that is, when the masses are at the cantilever tip is the most sensitive case since the value of the calibration constant is highest for this case. Therefore, for graphene based sensors in the cantilever configuration, it is desirable to place the mass at the free edge.

4. Numerical results and discussion

The nonlocal sensor equations derived in Section 3 are validated herewith. The nonlocal sensor equations are based on frequency shift of the SLGS. An armchair single layer graphene sheet of length 4.12 nm and width 2.21 nm is considered. Any other size would have been taken. The small size of the graphene layer considered in the numerical study is due to the computational limitation of the molecular mechanics method. A complete simulation with up to 10–12 different mass ratios for each of the four cases is significantly time consuming. Note that the proposed sensor equation (26) is based on nonlocal continuum theory and therefore is not limited to this small size. We expect that if the proposed sensor theory works for such a small scale, it is expected to work better for larger scale. The mass of the SLGS is 7.57 zeptogram ($1\,\text{zg} = 10^{-21}\,\text{g}$) and in the cantilever configuration its first natural frequency without small-scale effects is 23.96 GHz. We use an adenosine as the added bio-fragment. The adenosine is a nucleoside composed of a molecule of adenine attached to a ribose sugar molecule. Adenosines are important in biochemical processes. It helps in energy transfer as adenosine triphosphate (ATP) and adenosine diphosphate (ADP) as well as in signal transduction as cyclic adenosine monophosphate. It is also an inhibitory neurotransmitter, believed to play a role in promoting sleep and

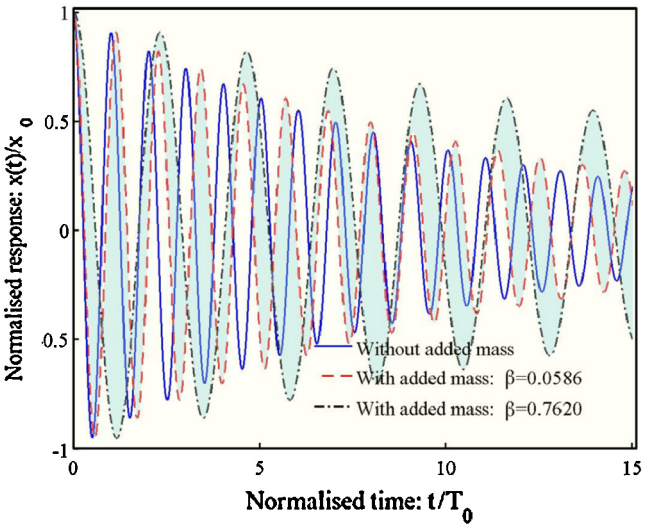

Fig. 4. Free vibration response at the tip of the graphene sheet due to the unit initial displacement obtained from molecular mechanics simulation. Here T_0 is the time period of oscillation without any added mass. The shaded area represents the motion of all the mass loading cases considered for case (a).

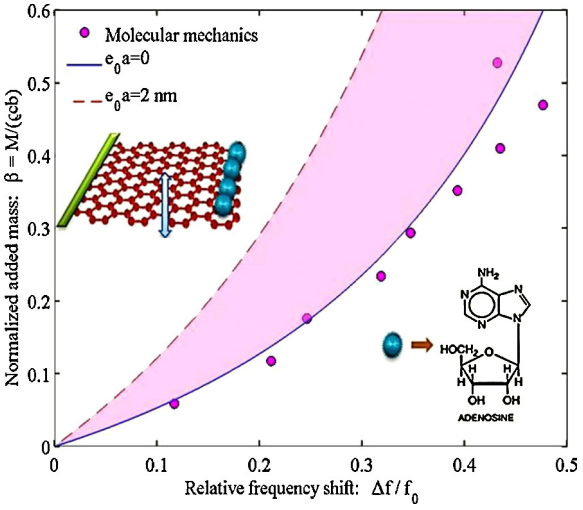

Fig. 5. Identified attached masses from the frequency-shift of a cantilevered SLGS resonator for case (a). The shaded area represents the results between the two possible extreme values of the nonlocal parameter. The SLGS mass is 7.57 zg and the mass of each adenosine molecule is 0.44 zg. The proposed approach is validated using data from the molecular mechanics simulations. Up to 9 adenosine molecules are attached to the graphene sheet.

suppressing arousal, with levels increasing with each hour an organism is awake.

In this paper we investigate the possibility of detecting Adenosine using a cantilevered single layer graphene sheet and nonlocal elasticity theory. The mass of each adenosine molecule is 0.44 zg, which is about 6% of the graphene mass. The Gaussian software in conjunction with the UFF model is used. Fig. 4 shows the normalised free vibration response at the tip of the graphene sheet due to unit initial displacement obtained from molecular mechanics simulation. Responses of the graphene sheet without and with added mass are shown. Here $T_0 = 2\pi/\Omega_0$ is the time period of oscillation without any added mass. A damping factor of 10% is considered for this plot. The shaded area represents the motion of all the mass loading cases considered. Added mass results the system to move slowly.

The added mass and the corresponding frequency-shift are determined from the molecular mechanics approach. Here the natural frequencies of the simple graphene sheet and graphene sheet with attached bio fragments are calculated. From these two sets of frequencies (with and without added mass), the frequency shifts are calculated. These frequency shifts in turn are considered as experimental observations and used in the nonlocal sensor Eq. (27). The magnitudes of the mass predicted by this equation are then compared with the known values used in the molecular mechanics simulations. The results from the molecular mechanics simulations are plotted as dots in the figure.

Since the nonlocal parameter in nonlocal plate theory is an important parameter and exact value is unknown, we choose a span for the value of parameter. We assume the range of parameter as from $e_0a = 0$–2 nm. When $e_0a = 0$, it represents the analysis based on classical sensor equations. When $e_0a > 0$ nm, it represents the analysis based on nonlocal sensor equations. Highly nonlocal case is represented when $e_0a = 2$ nm. In other words, this means that the stress at a point in the graphene is heavily influenced by the strains at all the other points. The analytical approach is verified with the exact approach in Fig. 5 for the case when the added molecules are at the cantilever tip in a line.

It can be seen that the results from the energy based analytical nonlocal approach are close to the molecular mechanics results for lower frequency shift. However it has to be noted that the small scale effects are less (i.e. smaller e_0a) for the present graphene sensor. The present analytical approach however deviates from the molecular mechanics results at higher relative frequencies shift (i.e. 0.4–0.6). This may be accounted for the fact that larger biofragment generates higher frequency shifts, and we have ignored the nonlocality due to the added mass. Thus for analytical approach with $e_0a = 2.0$ nm, the added mass and the frequency plot is away from the molecular mechanics results. The maximum sensitivity obtained from Eq. (30) without nonlocal effect is calculated as 6.9761 GHz/zg. Further when the added mass is very high (when mass ratio is more than 0.3); the proposed analytical approach becomes less accurate. For such high value of the added mass, the assumed deformation shape in Eq. (4) is not strictly applicable as it was derived for SLGS without any added mass. As a consequence the energy expressions and consequence the frequency estimate becomes inaccurate. This analysis without nonlocal effect showed that the proposed expressions are accurate up to added mass weighing 35% of the SLGS mass. Beyond this the proposed approach starts to lose accuracy. This may not be a severe limitation as 35% of the SLGS mass can be adequate for practical applications. If higher mass needs to be identified, one can simply use a larger SLGS within the sensor device. We therefore conclude that the mass of SLGS should be approximately more than 3 times the mass to be detected in order to reliably use the proposed analytical expressions.

Fig. 6 depicts the identified masses from the nonlocal frequency-shift for case (b), that is, when the added adenosine molecules are arranged in a line along the width. For the analytical calculation we consider $\gamma = 0.85$. The maximum sensitivity obtained form Eq. (30) and $e_0a = 0$ nm is calculated as 4.0992 GHz/zg.

It can be seen that, the results from the energy based nonlocal analytical approach match the exact results obtained from the molecular mechanics reasonably well. Most of the results within the span of analytical nonlocal elasticity cover the results from molecular mechanics approach. Unlike the local analytical approach, nonlocal analytical approach caters to majority of added mass generating different frequency ratios. Compared to the previous case it can also be seen that for a given value of added mass, the relative frequency shift is less for this case with and without nonlocal effects. This implies that the SLGS based sensor for this

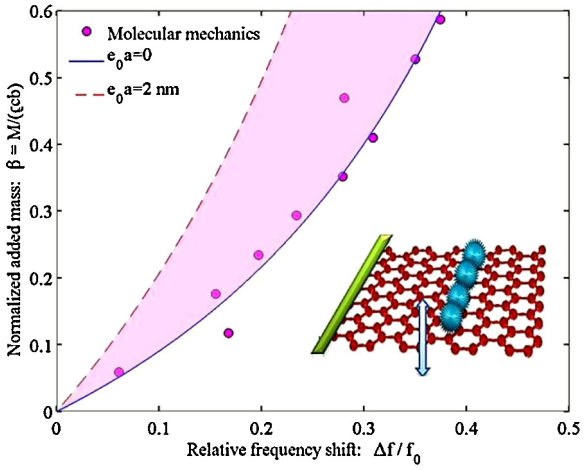

Fig. 6. Identified attached masses from the frequency-shift of a cantilevered SLGS resonator for case (b). The shaded area represents the results between the two possible extreme values of the nonlocal parameter. The proposed approach is validated using data from the molecular mechanics simulations. Up to 10 adenosine molecules are attached to the graphene sheet.

mass distribution is less sensitive compared to the case when the mass was placed at the edge.

Identified masses corresponding to case (c) are depicted in Fig. 7. In the figure we consider $\gamma = 0.25$ and $\eta = 0.6$. The maximum sensitivity obtained from Eq. (30) without nonlocal effects is calculated as 1.7401 GHz/zg. For this case the sensitivity is less and lowest compared to earlier cases. Without nonlocal effects, the proposed approach generally captures the trend of the added mass but the accuracy is lower compared to the last two cases. However considering nonlocal effects, the accuracy is good for lower frequency shifts. This shows the superiority of nonlocal sensor equations over the local sensor equations for graphene sensors.

Identified masses corresponding to case (d) are shown in Fig. 8. This is the most general case when the added masses are arranged in a line with an arbitrary angle. For the results shown in Fig. 6, we consider $\gamma = 0.25$, $\eta = 0.7$ and $\theta = \pi/6$. The maximum sensitivity obtained from Eq. (30) without nonlocal effects is

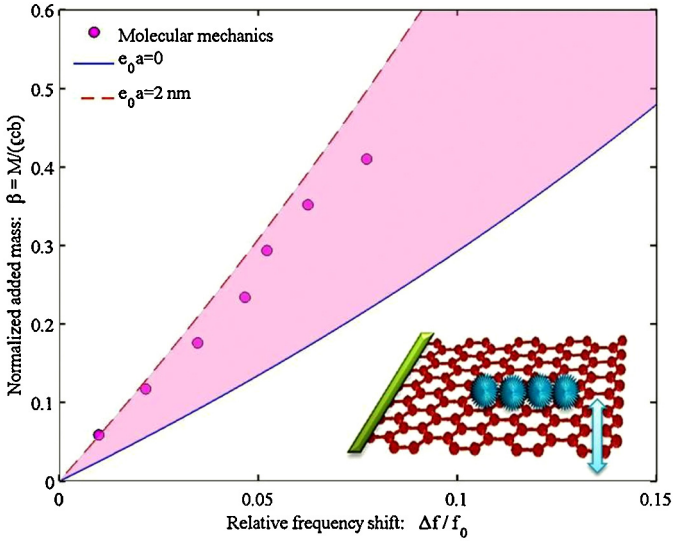

Fig. 7. Identified attached masses from the frequency-shift of a cantilevered SLGS resonator for case (c). The shaded area represents the results between the two possible extreme values of the nonlocal parameter. The proposed approach is validated using data from the molecular mechanics simulations. Up to 7 adenosine molecules are attached to the graphene sheet.

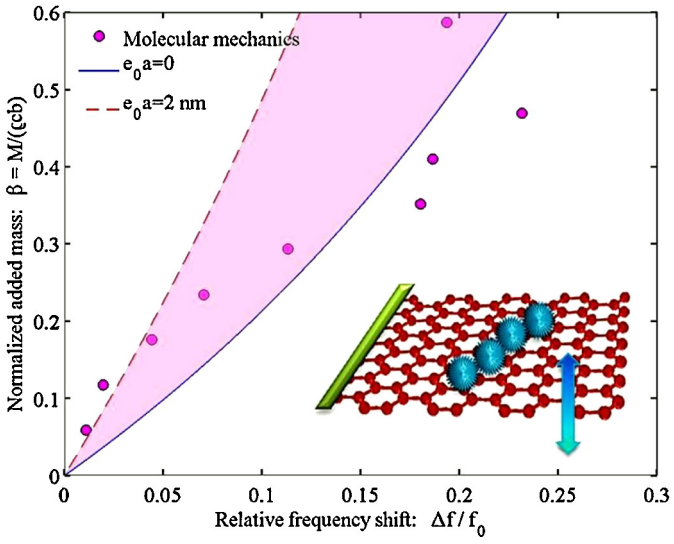

Fig. 8. Identified attached masses from the frequency-shift of a cantilevered SLGS resonator for case (d). The shaded area represents the results between the two possible extreme values of the nonlocal parameter. The proposed approach is validated using data from the molecular mechanics simulations. Up to 9 adenosine molecules are attached to the graphene sheet.

calculated as 1.7401 GHz/zg. The proposed approach generally captures the trend of the added mass with that of molecular mechanics approach. Here we can see that the nonlocal sensor equations cover most of the added mass compared to local sensor equations.

In summary in this paper an analytical method for calculating the frequency shift in a graphene based resonator is shown using nonlocal elasticity. Validation is carried out with molecular mechanics simulation results. Up to 60% of mass loading is considered in the numerical examples involving four possible loading patterns. In general the proposed nonlocal theory is accurate up to 35% of mass loading. The trend in resonating graphene sensors is to increase the sensitivity by making the resonators smaller. The theoretical model is reasonable, however it cannot be denied that many technological problems still, such as manufacturability, readout and functionalisation are present. The work presented here could act as an input to understand such graphene sensors once they become realisable. This is a case where the theory might be ahead of the fabrication capabilities, but it will be a valuable model to have for evaluating future cantilever graphene sensors.

5. Conclusions

In this paper, we theoretically investigate the application of nonlocal elasticity for the possibility of using single layer graphene sheet (SLGS) as a nanoscale label free mass sensor. Nonlocal theory is appropriate theory as it considers small-scale effects at nanoscale such as in graphene. The shift in the resonance frequencies obtained via nonlocal sensor equations due to the additional mass is exploited in the proposed sensor. The SLGS resonator is assumed to be in cantilevered configuration. Four physically realistic mass distributions are addressed. These comprise masses at the (i) cantilever tip in a line, (i) masses in a line along the width, (iii) masses in a line along the length and (iv) masses in a line with an arbitrary angle. Since the nonlocal parameter in nonlocal elasticity is an important parameter and exact value is unknown, we choose a span for the value of parameter. This comprises analysis without nonlocal effects too. It is observed that the performance of the sensor depends on the spatial distribution of the attached mass on the graphene sheet with and without nonlocal effects. Explicit closed-form nonlocal analytical expressions have been derived to

detect the added mass from the frequency shift. Sensitivities of the proposed sensor for different mass distributions are compared. A molecular mechanics based approach is used to validate the analytical sensor equations. We used the UFF force field model, wherein the force field parameters are estimated using the general rules based on the element, its hybridisation and its connectivity. Acceptable agreements between the proposed approach and the molecular mechanics simulations have been observed.

Numerical results indicate that the new equations derived in the paper are acceptable when the added mass is up to 1/3 of the mass of the SLGS cantilever without nonlocal effects. Our analysis shows that by placing the adenosine at the edge of the graphene sheet results in the most sensitive sensor. This observation is related to the modal profile of the graphene, i.e. that a mass at the tip is moving up and down more vigorously than a mass at a different position. Further research will include the dynamics of the subgrade which is essential for immobilising the bio-molecules on to the graphene sheets. For some cases i.e. external masses at the cantilever tip in a line and in a line along the width of graphene, the classical local model can be used with very good accuracy. Cases of graphene sensor with additional masses in a line along the length and in a line with an arbitrary angle, on the other hand, show strong nonlocal effect. Since the nonlocal elasticity approach is more general and consider the classical local elasticity as a special case, the sensors equations derived here can be used for all the four cases in general. Significant work is also necessary to physically realise a graphene based mass sensing resonator where the analytical nonlocal expressions developed in this paper would be utilised.

Acknowledgements

S.A. and T.M. acknowledge the support of Royal Society through the award of Wolfson Research Merit award and Irish Research Council, respectively.

References

[1] A. Geim, K. Novoselov, Nature Materials 6 (2007) 183.
[2] Y. Hancock, Journal of Physics D: Applied Physics 44 (2011) 473001.
[3] Y. Huang, J. Wu, K. Hwang, Physical Review B 74 (2006) 245413.
[4] S. Kim, H. Park, Journal of Applied Physics 110 (2011) 054324.
[5] L. Lin, D. Kim, W. Kim, S. Jun, Surface & Coatings Technology 205 (2011) 4864.
[6] L. Yang, C. Park, Y. Son, M. Cohen, S. Louie, Physical Review Letters 99 (2007) 186801.
[7] S. IIJIMA, Nature 354 (1991) 56.
[8] J. Moon, D. Gaskill, IEEE Transactions on Microwave Theory and Techniques 59 (2011) 2702.
[9] M. Sima, I. Enculescu, A. Sima, Optoelectronics and Advanced Materials – Rapid Communications 5 (2011) 414.
[10] S. Chu, L. Hu, X. Hu, M. Yang, J. Deng, International Journal of Hydrogen Energy 36 (2011) 12324.
[11] L. Grande, V. Chundi, D. Wei, C. Bower, P. Andrew, T. Ryhanen, Particuology 10 (2012) 1.
[12] Y. Shao, J. Wang, H. Wu, J. Liu, I. Aksay, Y. Lin, Electroanalysis 22 (2010) 1027.
[13] P. Ang, W. Chen, A. Wee, K. Loh, Journal of the American Chemical Society 130 (2008) 14392.
[14] T. Murmu, S. Adhikari, Sensors and Actuators A: Physical 173 (2012) 41.
[15] B. Zhang, Q. Li, T. Cui, Biosensors & Bioelectronics 31 (2012) 105.
[16] L. Feng, L. Wu, J. Wang, J. Ren, D. Miyoshi, N. Sugimoto, X. Qu, Advanced Materials 24 (2012) 125.
[17] F. Yavari, Z. Chen, A. Thomas, W. Ren, H. Cheng, N. Koratkar, Scientific Reports 1 (2011) 166.
[18] A. Sakhaee-Pour, M. Ahmadian, A. Vafai, Solid State Communications 145 (2008) 168.
[19] I. Kang, H. So, G. Bang, J. Kwak, J. Lee, C. Ahn, Applied Physics Letters 101 (2012) 123504.
[20] K. Ratinac, W. Yang, S. Ringer, F. Braet, Environmental Science & Technology 44 (2010) 1167.
[21] T. Gan, S. Hu, Microchimica Acta 175 (2011) 1.
[22] V. Sorkin, Y. Zhang, Journal of Molecular Modeling 17 (2011) 2825.
[23] S. Pisana, P. Braganca, E. Marinero, B. Gurney, IEEE Transactions on Magnetics 46 (2010) 1910.
[24] J. Jiang, J. Wang, B. Li, Physical Review B 80 (2009) 113405.
[25] T. Han, P. He, J. Wang, A. Wu, New Carbon Materials 25 (2010) 261.
[26] B. Akgoz, O. Civalek, Materials & Design 42 (2012) 164.
[27] A. Eringen, Journal of Applied Physics 54 (1983) 4703.
[28] S. Bauer, A. Pittrof, H. Tsuchiya, P. Schmuki, Electrochemistry Communications 13 (2011) 538.
[29] M. Kahrobaiyan, M. Asghari, M. Rahaeifard, M. Ahmadian, International Journal of Engineering Science 48 (2010) 1985.
[30] C. Kiang, M. Endo, P. Ajayan, G. Dresselhaus, M. Dresselhaus, Physical Review Letters 81 (1998) 1869.
[31] M. Aydogdu, Physica E – Low-Dimensional Systems & Nanostructures 41 (2009) 861.
[32] J. Hsu, H. Lee, W. Chang, Current Applied Physics 11 (2011) 1384.
[33] H. Babaei, A. Shahidi, Archive of Applied Mechanics 81 (2011) 1051.
[34] C. Wang, W. Duan, Journal of Applied Physics 104 (2008) 014303.
[35] R. Artan, A. Tepe, Mechanics of Advanced Materials and Structures 18 (2011) 347.
[36] T. Murmu, S.C. Pradhan, Journal of Applied Physics 105 (2009) 064319.
[37] J. Yang, X. Jia, S. Kitipornchai, Journal of Physics D: Applied Physics 41 (2008) 035103.
[38] H. Heireche, A. Tounsi, H. Benhassaini, A. Benzair, M. Bendahmane, M. Missouri, S. Mokadem, Physica E – Low-Dimensional Systems & Nanostructures 42 (2010) 2375.
[39] B. Arash, Q. Wang, Computational Materials Science 51 (2012) 303.
[40] H. Lee, J. Hsu, W. Chang, Nanoscale Research Letters 5 (2010) 1774.
[41] Z.-B. Shen, B. Deng, X.-F. Li, G.-J. Tang, Journal of Nanotechnology in Engineering and Medicine 2 (2012) 031003.
[42] M. Aydogdu, S. Filiz, Physica E – Low-Dimensional Systems & Nanostructures 43 (2011) 1229.
[43] Z. Shen, H. Tang, D. Li, G. Tang, Computational Materials Science 61 (2012) 200.
[44] J. Bunch, A. van der Zande, S. Verbridge, I. Frank, D. Tanenbaum, J. Parpia, H. Craighead, P. McEuen, Science 315 (2007) 490.
[45] S. Adhikari, R. Chowdhury, Physica E – Low-Dimensional Systems & Nanostructures 44 (2012) 1528.
[46] K. Eom, H. Park, D. Yoon, T. Kwon, Physics Reports – Review Section of Physics Letters 503 (2011) 115.
[47] K. Ekinci, Y. Yang, M. Roukes, Journal of Applied Physics 95 (2004) 2682.
[48] J. Chaste, A. Eichler, J. Moser, G. Ceballos, R. Rurali, A. Bachtold, Nature Nanotechnology 7 (2012) 300.
[49] R. Chowdhury, S. Adhikari, C. Wang, F. Scarpa, Computational Materials Science 48 (2010) 730.
[50] S. Pradhan, J. Phadikar, Physics Letters A 373 (2009) 1062.
[51] R. Ansari, S. Sahmani, B. Arash, Physics Letters A 375 (2010) 53.
[52] R. Ansari, B. Arash, H. Rouhi, Composite Structures 93 (2011) 2419.
[53] T. Aksencer, M. Aydogdu, Physica E – Low-Dimensional Systems & Nanostructures 43 (2011) 954.
[54] R. Ansari, R. Rajabiehfard, B. Arash, Computational Materials Science 49 (2010) 831.
[55] W. Duan, C. Wang, Y. Zhang, Journal of Applied Physics 101 (2007).
[56] S. Narendar, S. Gopalakrishnan, Journal of Applied Mechanics – Transactions of the ASME 78 (2011) 061018.
[57] R.D. Blevins, Formulas for Natural Frequency and Mode Shape, Krieger Publishing Company, Malabar, FL, USA, 1984.
[58] J. Meyer, A. Geim, M. Katsnelson, K. Novoselov, T. Booth, S. Roth, Nature 446 (2007) 60.
[59] V. Shenoy, C. Reddy, A. Ramasubramaniam, Y. Zhang, Physical Review Letters 101 (2008).
[60] B. Huang, M. Liu, N. Su, J. Wu, W. Duan, B. Gu, F. Liu, Physical Review Letters 102 (2009) 166404.
[61] A. Gil, S. Adhikari, F. Scarpa, J. Bonet, Journal of Physics: Condensed Matter 22 (2010) 145302.
[62] S. Adali, Acta Mathematica Scientia 32 (2012) 325.
[63] C. Chen, S. Rosenblatt, K. Bolotin, W. Kalb, P. Kim, I. Kymissis, H. Stormer, T. Heinz, J. Hone, Nature Nanotechnology 4 (2009) 861.

Biographies

Dr. Tony Murmu (T. Murmu) is an Empower Research Fellow (Irish Research Council) in the University of Limerick, Republic of Ireland. He received his PhD (2010) in Aerospace Engineering from Indian Institute of Technology (IIT), Kharagpur, India. He obtained his Master's of Mechanical Engineering (M.M.E) from Jadavpur University, Kolkata, India in 2006. After PhD he worked as a Researcher in Civil and Computational Engineering Centre, College of Engineering, Swansea University, UK. His research interests include nonlocal elasticity, carbon nanotubes, graphene sheets and scale dependent theories for nano-mechanical systems.

Dr. Sondipon Adhikari (S. Adhikari) is a Full Professor in the College of Engineering in Swansea University, UK. He received his PhD (2001) from Cambridge University (Trinity College). He was a Research Fellow in Fitzwilliam College, Cambridge and Lecturer in Bristol University prior to this position. His research interest includes dynamical systems, stochastic methods, nano and bio mechanics.